Chemistry & Biology
Article

Identification of the Viridicatumtoxin and Griseofulvin Gene Clusters from *Penicillium aethiopicum*

Yit-Heng Chooi,[1] Ralph Cacho,[1] and Yi Tang[1,*]
[1]Department of Chemical and Biomolecular Engineering, University of California, Los Angeles, Los Angeles, CA 90095, USA
*Correspondence: yitang@ucla.edu
DOI 10.1016/j.chembiol.2010.03.015

SUMMARY

Penicillium aethiopicum **produces two structurally interesting and biologically active polyketides: the tetracycline-like viridicatumtoxin 1 and the classic antifungal agent griseofulvin 2. Here, we report the concurrent discovery of the two corresponding biosynthetic gene clusters (*vrt* and *gsf*) by 454 shotgun sequencing. Gene deletions confirmed that two nonreducing PKSs (NRPKSs), *vrtA* and *gsfA*, are required for the biosynthesis of 1 and 2, respectively. Both PKSs share similar domain architectures and lack a C-terminal thioesterase domain. We identified *gsfI* as the chlorinase involved in the biosynthesis of 2, because deletion of *gsfI* resulted in the accumulation of decholorogriseofulvin 3. Comparative analysis with the *P. chrysogenum* genome revealed that both clusters are embedded within conserved syntenic regions of *P. aethiopicum* chromosomes. Discovery of the *vrt* and *gsf* clusters provided the basis for genetic and biochemical studies of the pathways.**

INTRODUCTION

Fungal polyketides are an important class of secondary metabolites, which include blockbuster drugs, mycotoxins, and pigments. There has been a growing interest in the engineering and heterologous expression of fungal polyketide synthase (PKS) genes and pathways to enable rational production of novel compounds (Schümann and Hertweck, 2006). Understanding the molecular genetic basis of the biosynthesis of these structurally diverse compounds is the underlying key to achieve this goal. Over the past decade, there has been a steady growth of knowledge on the mechanisms of fungal polyketide biosynthetic pathways (Cox, 2007). Numerous fungal polyketides have been linked to their PKS genes and gene clusters (Hoffmeister and Keller, 2007), including some from the cryptic metabolic pathways uncovered via genome mining (Bergmann et al., 2007; Bok et al., 2006; Chiang et al., 2008). Nevertheless, the biosynthetic pathways of many previously known fungal metabolites, some of which have important pharmaceutical applications, still remain to be elucidated.

The filamentous fungus *Penicillium aethiopicum* Frisvad is known to produce a number of interesting secondary metabolites, including viridicatumtoxin (**1**), griseofulvin (**2**), and tryptoquialanine (**4**) (Figure 1), which are used as chemotaxonomic markers for the species (Frisvad and Samson, 2004). Tryptoquialanine is a tetrapeptide structurally similar to tryptoquivaline, which is a known tremorgen (Ariza et al., 2002; Clardy et al., 1975). Viridicatumtoxin is a hybrid polyketide-isoprenoid compound and is a rare example of tetracycline-like compounds produced by fungi. Compound **1** shares a common tetracyclic carboxamide core with the well-known tetracycline intermediate anhydrotetracycline; **1** has been reported to cause nephrotoxicity (Hutchison et al., 1973) as well as exhibiting modest antitumor activity (Raju et al., 2004). An epoxide derivative of the compound, viridicatumtoxin B, was isolated from *Penicillium* species FR11 along with **1**; both were shown to inhibit the growth of methicilin- and quinolone-resistant *Staphylococcus aureus* at 8–64 times higher activity than tetracycline (Zheng et al., 2008). Another known fungal compound with a tetracyclic carboxamide core is anthrotainin (TAN-1652) (Ishimaru et al., 1993; Wong et al., 1993), which is an inhibitor of neuropeptide substance P binding and is a potential nonsteroidal anti-inflammatory agent. The biosynthetic convergence of tetracycline-like compounds across the bacterial and fungal kingdoms, and their various bioactivities, further suggest that compounds of this structural type contain an "evolutionarily privileged scaffold," which is capable of interacting with a variety of biological targets. The co-occurrence of tetracyclic carboxamide core in both the tetracyclines from bacteria and **1** from fungi provides an excellent example to study the convergence of the polyketide pathway. Previous isotope feeding study (de Jesus et al., 1982) showed that **1** is produced by a mechanism significantly different from the bacterial tetracyclines (Thomas, 2001). The formation and attachment of the spirobicyclic ring of isoprenoid origin on a tetracycline scaffold also warrants detailed biosynthetic investigation.

Griseofulvin, which affects the function of mitotic spindle microtubules in mitosis, is an antifungal drug and has been in use for many years in medical and veterinary applications (Finkelstein et al., 1996). Although the use of **2** is mostly superseded by newer and more effective synthetic antifungal agents, it remains useful for the treatment of some dermatophytes, such as *Tinea capitis* (ringworm of the scalp) and *Tinea pedis* (athlete's foot). Recently, there has been a renewed interest in **2** owing to its specific antiproliferative and antimitotic activities toward cancer cells (Panda et al., 2005; Rebacz et al., 2007). The recent

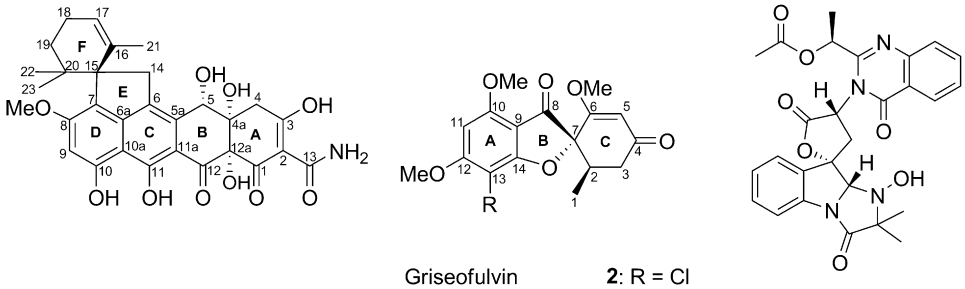

Figure 1. Structures of the Major Secondary Metabolites Produced by *P. aethiopicum*
The numbering schemes for the carbon atoms for **1-3** are based on previous studies (de Jesus et al., 1982; Simpson and Holker, 1977).

studies suggest that **2** acts by inhibiting centrosomal clustering in tumor cells with supernumerary centrosomes, causing multipolar mitoses, and subsequently, apoptosis (Rebacz et al., 2007). Interestingly, **2** has also been shown to suppress hepatitis C virus replication in vitro (Jin et al., 2008). The discovery of the new potentials of **2** has led to new synthetic efforts to search for superior analogs (Rønnest et al., 2009). Structurally, **2** has an interesting cyclization pattern, where the polyketide backbone is folded to allow formation of orcinol and phloroglucinol ring structures through a Claisen and an aldol reactions, respectively. A stereospecific oxidative coupling reaction was proposed for the formation of the grisan structure of **2** (Barton and Cohen, 1957). The biosynthetic pathway of **2** has been extensively studied using isotopic incorporation (Harris et al., 1976; Lane et al., 1982; Rhodes et al., 1963; Simpson and Holker, 1977), but the genes and enzymes involved in the biosynthesis remain unknown.

The significant biological properties and unusual structural features of **1** and **2** have motivated us to perform a genome scanning of *P. aethiopicum* with DNA pyrosequencing technology and search for the two corresponding gene clusters. A bioinformatic search for PKS genes and comparative analysis with *Penicillium chrysogenum* genome revealed the putative biosynthetic gene clusters for both compounds, which were confirmed by targeted gene deletions and RNA silencing. The two gene clusters provide an important step toward understanding the enzymatic basis of biosynthesis of **1** and **2**.

RESULTS AND DISCUSSION

Genome-Wide Analysis of *P. aethiopicum* PKS Genes Revealed Two Putative Gene Clusters for Viridicatumtoxin and Griseofulvin Biosynthesis

The 454 shotgun sequencing of *P. aethiopicum* IBT 5753 with the GS FLX Titanium series generated a total of ~572 million bases with an average sequencing read length of 367.5 bases. Assembly of the unpaired shotgun sequence reads resulted in 1522 contigs, which consist of 28,925,551 nonredundant bases, with an N50 of 149.2 kb. On the basis of the phylogenetic analysis of β-tubulin sequences, *P. aethiopicum* is closely related to *P. chrysogenum*, and both species are grouped under *Penicillium* subgenus *Penicillium*, section *Chrysogena* (Samson et al., 2004). Assuming that the size of *P. aethiopicum* genome is close to that of the sequenced *P. chrysogenum* genome (32.19 Mb), the total nonredundant bases were estimated to cover about 90% of the fungal genome.

Using a local BLASTP program queried against a database consisting of all the contigs with an arbitrary ketosynthase (KS) domain sequences, a total of 30 putative, complete PKS genes were found in the *P. aethiopicum* genome. Out of the 30 genes, there are a total of seven nonreducing PKSs (NRPKSs), 17 highly reducing PKSs (HRPKS), three partially reducing PKSs (PRPKSs), and three HRPKS-nonribosomal peptide synthetases (NRPSs) hybrids. For simplicity, the PKSs are designated as PaPKS[contig number] (see Table S1 available online).

Compared with *P. chrysogenum*, which has a total of 21 putative PKS genes, the *P. aethiopicum* genome contains more putative PKS genes. According to a chemotaxonomic study, the two closely related species are known to produce distinct sets of secondary metabolites (Frisvad and Samson, 2004). Because *P. chrysogenum* is not known to produce **1** and **2**, we reasoned that the orthologous PKSs are not involved in the biosynthesis of the two compounds. Sequence alignments and phylogenetic analysis implied that nine out of the 30 putative PKS genes in *P. aethiopicum* are orthologous to *P. chrysogenum* (Table S1 and Figure S1).

We reasoned that NRPKSs are likely involved in the biosynthesis of the carbon skeletons of **1** and **2**, because these compounds are derived from aromatic polyketide precursors. Among the *P. aethiopicum* NRPKSs that are nonorthologous to those found in *P. chrysogenum,* PaPKS0274 and PaPKS0880 fall into the same clade as the recently identified *Aspergillus nidulans* asperthecin synthase (AptA) (Szewczyk et al., 2008) and *Aspergillus terreus* atrochrysone carboxylic acid synthase (ACAS) (Awakawa et al., 2009), both of which produce fused-ring aromatic compounds (Figure S1). Both PaPKS0274 and PaPKS0880 consist of starter unit:ACP transacylase (SAT) (Crawford et al., 2006), KS, malonyl-CoA:ACP transacylase (MAT), product template (PT) (Crawford et al., 2009), and acyl carrier protein (ACP) domains, but lack a thioesterase/Claisen cyclase (TE/CLC) domain (Fujii et al., 2001) at the C-terminal for chain release. Because the ACAS product, atrochrysone carboxylic acid, has a structure similar to that of the BCD rings of **1**, we predicted that one of these two PKSs may be involved in the biosynthesis of **1**.

Given that genes involved in fungal secondary metabolic pathways are often clustered together (Hoffmeister and Keller, 2007), we searched the genes surrounding the two putative PKS genes

for clues about the final polyketide products. Preliminary bioinformatic analysis of contig 00274 identified a pair of genes related to isoprenoid pathway downstream of PaPKS0274 gene. The presence of both genes may be associated with the isoprenoid portion of the spirobicyclic ring in **1**. Other genes encoding putative oxygenases, aminotransferase, and *O*-methyltransferase were also found in the vicinity of the PaPKS0274 gene, which respectively match the structural features present in **1**. On contig 00880, the presence of three putative *O*-methyltransferase genes and a halogenase gene flanking the PaPKS0880 gene immediately points to a potential correlation to the structure of **2**.

VrtA and GsfA Are Two PKSs Essential for the Biosynthesis of Viridicatumtoxin and Griseofulvin, Respectively

Liquid chromatography–mass spectrometry (LC-MS) analysis of the ethyl acetate extract from *P. aethiopicum* wild-type (WT) stationary culture grown in yeast malt extract glucose (YMEG) medium showed six distinct peaks at 283 nm. Two of the peaks have the retention time, UV spectra, and *m/z* value matching the authentic standards of **1** (RT = 30 min, *m/z* 548 $[M+H-H_2O]^+$) and **2** (RT = 24 min, *m/z* 353 $[M+H]^+$) (Figure 2). Another peak at RT = 22 min showed a UV spectrum that is similar to that of **2** and *m/z* 319 $[M+H]^+$, which matches with the molecular weight of dechlorogriseofulvin **3** (Figure 1). The compound was purified from a large culture of *P. aethiopicum*, and the structure was confirmed to be **3** by comparing the ^1H NMR and ^{13}C NMR spectra to the previously published spectra for **2** (Simpson and Holker, 1977) and epidechlorogriseofulvin (Jarvis et al., 1996) (Table S3). Two additional peaks (RT = 27 and 28 min) with UV spectra similar to previously reported for tryptoquivalines and tryptoquialanines were also detected (Ariza et al., 2002; Clardy et al., 1975). Both peaks have a mass of $[M+H]^+$ *m/z* = 519, which matches with the molecular weight of **4**. The additional peak could be an isomer of **4**, analogous to tryptoquivaline and isotryptoquivaline (Yamazaki et al., 1976). The identity of the remaining peak at RT = 19.5 min is undetermined.

To verify the proposed associations between the putative gene clusters and the metabolites **1** and **2,** we developed a transformation system for *P. aethiopicum* based on existing methods for *A. nidulans* using *bar* resistant marker (Chooi et al., 2008; Nayak et al., 2006). Using double-homologous deletion cassettes with a *bar* resistant marker, the PaPKS0274 and PaPKS0880 genes were deleted by double crossover recombination (Figure 3). Approximately 100 glufosinate-resistant transformants were picked and screened with PCR using a *bar* gene primer and primers outside of the deletion cassette (Table S2). A total of six and five potential recombinants were identified for PaPKS0274 and PaPKS880, respectively. Three PCR-positive clones from each knockout experiments were chosen and confirmed by Southern hybridization (Figure 3). All the PCR-positive clones (ΔPKS0274-I16, ΔPKS0274-I18, ΔPKS0274-I23, ΔPKS880-I7, ΔPKS880-I12, and ΔPKS880-I9) showed the expected band size for correct insertion of deletion cassette by double crossover recombination into the corresponding genomic copy of the two PKS genes. Analysis of the PaPKS0274 disruptants showed that the production of **1** was totally abolished (Figure 2), whereas the other metabolites were unaffected.

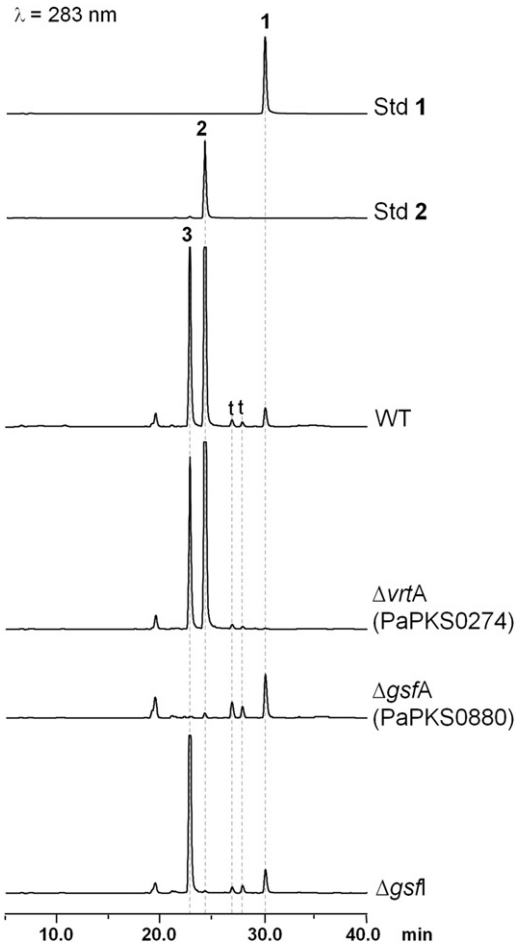

Figure 2. HPLC Analysis (283 nm) of Metabolites Produced by Wild-Type and Mutant *P.aethiopicum* Strains

The mutant Δ*vrtA,* Δ*gsfA*, or Δ*gsfI* no longer produced **1, 2** or **3**, respectively. Standards of compounds **1** and **2** are shown. The identity of **3** was established by NMR characterization. Peaks labeled with **t** have UV spectra and *m/z* values matching to **4** and can be isomers.

For the PaPKS0880 disruptants, only the production of **2** and **3** were abolished (Figure 2). These results confirmed that PaPKS0274 is essential for the biosynthesis of **1**, whereas PaPKS0880 is required for the biosynthesis of **2** and **3**.

The two PKS gene clusters for **1** and **2** were designated as *vrt* and *gsf*, respectively, and the two NRPKS genes were designated as *vrtA* and *gsfA*, respectively (Tables 1 and 2). Interestingly, both PKSs have the same domain architecture and lack a fused TE/CLC domain. The functional assignment of VrtA and GsfA, which produce polyketides with different chain lengths and backbone folding patterns in **1** and **2**, suggested that this family of "TE-less" PKSs (assigned as clade IV NR-PKSs here) (Figure S1) may account for a greater structural diversity among fungal polyketides.

We also tested whether the production of **1** and **2** in *P. aethiopicum* can be attenuated or abolished by using RNA silencing. This strategy has been previously used in the identification of the chaetoglobosin gene cluster from *P. expansum* (Schumann and Hertweck, 2007) and in the study of tailoring oxidations

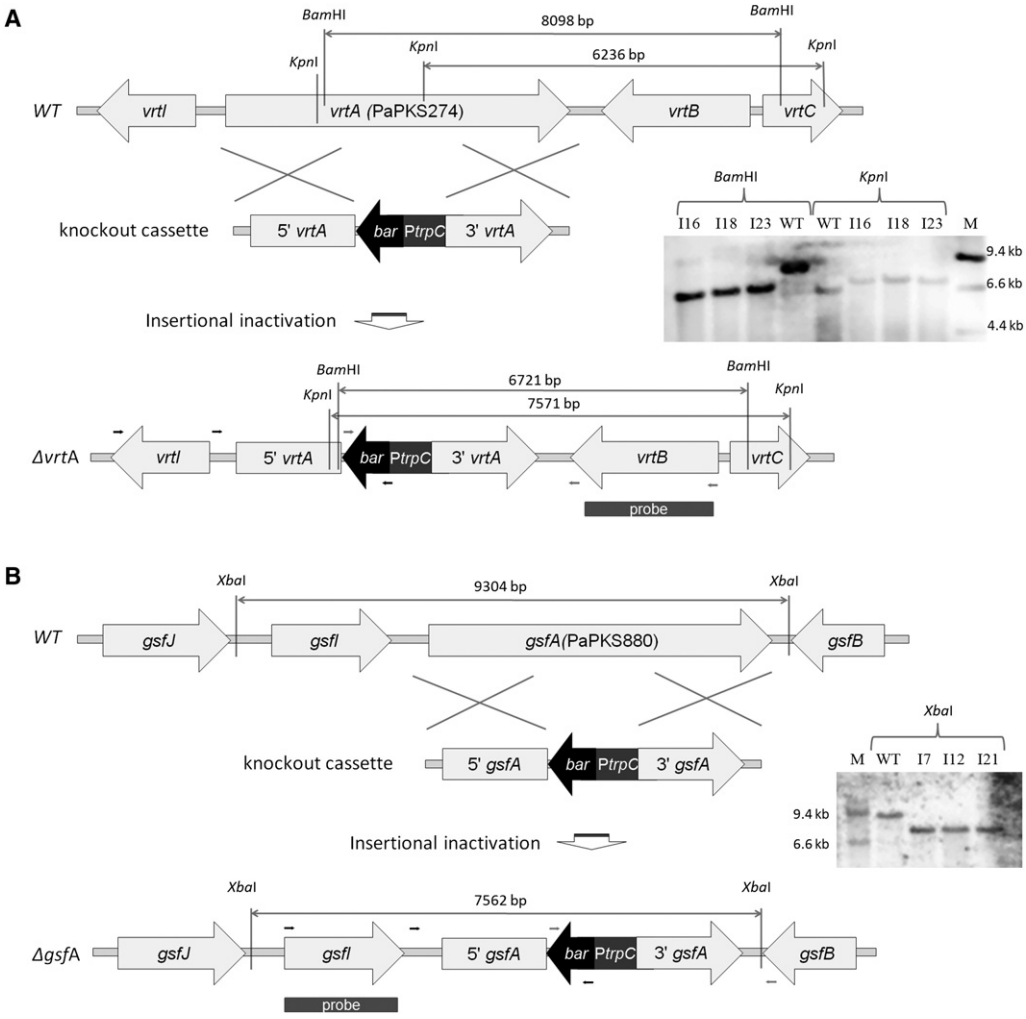

Figure 3. Homologous Recombination Schemes for Deletion of *vrtA* and *gsfA* Genes in *P. aethiopicum*

The knockout cassettes for *vrtA* (PaPKS0274) (A) and *gsfA* (PaPKS880) (B) are shown with marked restriction sites. The corresponding Southern blot results for the wild-type and the mutants are displayed on the right. Small arrows indicate approximate binding sites of the primers used in PCR screening.

during tenellin biosynthesis in *Beauveria bassiana* (Halo et al., 2008). Gene fragments of PaPKS0274 (3.8 kB) and PaPKS0880 (2.5 kB) were separately cloned into the pBARGPE1 plasmid (Pall and Brunelli, 1993) in the antisense orientation under the control of a *gpdA* promoter. The resultant plasmids, pBAR274si and pBAR880si, were randomly integrated into the *P. aethiopicum* genome. We recovered nine clones for PaPKS0274 and six clones for PaPKS0880 that contain the full length *gpdA* promoter with contiguous PKS gene fragments. For the *vrtA* silencing, three of the nine PCR-positive clones screened did not produce **1**, whereas the other six clones showed various degree of reduced viridicatumtoxin production compared to wild-type (Figure S2). In the case of *gsfA*, all six clones continued to produce **2** and **3**, but at various lower titers compared to wild-type (Figure S3). The level of silencing of the two PKS genes is likely linked to the copy number of the silencing constructs integrated in the transformants, the expression level of the antisense gene driven by the *gpdA* promoter, and the endogenous transcript levels of the two corresponding PKS genes. The inability to silence *gsfA* completely may due to the high level of endogenous gene expression, as reflected in the relatively large amount of **2** produced in the culture.

Comparative Genomics Analysis Revealed the *vrt* and *gsf* Cluster Embedded Within Conserved Syntenic Regions of *P. aethiopicum* Genome

A more detailed bioinformatic analysis of the two biosynthetic loci revealed adjacent genes that are highly similar and syntenic to those found in *P. chrysogenum* genome (80%–99% identity). Except for the regions surrounding *vrtA* and *gsfA*, the conserved syntenic blocks span the whole contig 0274 and 0880, and they correspond to a specific locus in *P. chrysogenum* contig Pc00c21 and Pc00c06, respectively (Figure 4). Under the assumption that secondary metabolic genes could be unique to individual species while housekeeping and primary metabolic genes are usually conserved among closely related organisms, we used those syntenic sets of orthologous genes to tentatively assign the boundaries of the two putative clusters (Figure 4).

Table 1. Putative Genes Within and Flanking the *vrt* Cluster

Gene	Size (bp/aa)	BLASTP homolog	Identity/ Similarity (%)	Conserved Domain	E value
vrtA	5578/1824	*A. nidulans*, AN6000.3 (AptA)	60/75	SAT-KS-MAT-PT-ACP	
vrtB	2312/723	*Pyrenophora tritici-repentis*, PTRG_06131 *Rattus norvegicus,* AACS_RAT	51/64 40/56	PRK03584, acetoacetyl-CoA synthetase	<1.0e-180
vrtC	1452/483	*Microsporum canis*, MCYG_03599 *A. fumigatus*, FgaPT2 [3I4X]	45/59 20/36	TIGR03429, aromatic prenyltransferase	2e-73
vrtD	1206/349	*Neurospora crassa,* FACPS_NEUCR [Q92250]	54/68	cd00685, trans-isoprenyl diphosphate synthases	7e-46
vrtE	1898/520	*A. terreus*, ATEG_04107	33/52	pfam00067, cytochrome P450	5e-24
vrtF	717/238	*A. niger*, An11 g07340 *Polyangium cellulosum*, JerF	55/65 35/49	pfam08242, methyltransferase domain type 12	1e-04
vrtG	924/307	*A. nidulans*, AN6001.3 (AptB)	60/74	smart00849, metallo-β-lactamase superfamily	2e-24
vrtH	1305/413	*A. nidulans*, AN6002.3 (AptC)	50/69	COG0654, UbiH and related FAD-dependent oxidoreductases	4e-11
vrtI	1597/413	*A. clavatus*, ACLA_098360 *Nicotiana tabacum,* Ntc12 gibberillin 20-oxidase	39/50 18/35	COG3491, PcbC, IPNS and related dioxygenases pfam03171, 2OG-Fe(II) oxygenase	2e27 2e-11
vrtJ	1249/388	*Sclerotinia sclerotiorum*, SS1G_01438 *Candida albicans*, Gly1 [GLY1_CANAL][6]	47/61 37/53	cd06502, low-specificity threonine aldolase (TA), PLP-dependent aspartate aminotransferase superfamily (fold I) pfam01212, Beta-eliminating lyase	1e-77 4e-70
vrtK	1847/534	*A. flavus, verB* desaturase *A. nidulans, stcL* desaturase	37/54 31/47	pfam00067, p450, Cytochrome P450	3e-41
vrtL	1570/503	*A. niger*, An13 g00720	80/89	cd06174, MFS, The Major Facilitator Superfamily transporters	1e-31
vrtR1	2148/715	*Neosartorya fischeri*, NFIA_025860	70/81	pfam04082, fungal specific transcription factor domain	2e-09
vrtR2	2757/836	*A. niger,*An11 g07350	34/48	smart00066, GAL4-like Zn(II)2Cys6 binuclear cluster DNA-binding domain	2e-05
orf1	789/262	*P. chrysogenum*, Pc21 g16760	91/95	COG0400, Predicted esterase	8e-12
orf2	444/147	*P. chrysogenum*, Pc21 g16750	99/100	No conserved domain detected	
orf3	675/224	*P. chrysogenum*, Pc21 g16710	93/95	COG4297, uncharacterized protein with double-stranded beta helix domain	3e-14
orf4	1974/657	*P. chrysogenum*, Pc21 g16680	92/94	No putative conserved domains detected	
orf5	1499/462	*P. chrysogenum*, Pc21 g16670	85/92	cd05120, aminoglycoside 3′-phosphotransferase (APH) and choline kinase (ChoK) family.	1e-04
orf6	1722/573	*Uncinocarpus reesii*, UREG_05338	26/40	cd00204, ANK, ankyrin repeats; mediate protein-protein interactions	0.004
orf7	888/263	*P. chrysogenum*, Pc21 g16640	97/99	pfam09177, Syntaxin 6, N-terminal pfam05739, SNARE domain	2e-21 2e-08
orf8	1112/319	*P. chrysogenum*, Pc21 g16630	95/98	pfam00956, NAP, Nucleosome assembly protein	1e-09

Genus abbreviation: A. -*Aspergillus*, P. - *Penicillium*.

In the case of the *vrt* gene cluster, 14 putative genes (designated as *vrtA-L*, *vrtR1*, and *vrtR2*) were found between *orf3* and *orf4*, which share 93% and 92% identity to Pc21 g16710 and Pc21 g16780, respectively (Figure 4A and Table 1). Most of the genes upstream of *orf3* and downstream of *orf4* also share syntenies and high similarities with genes in the corresponding locus on the *P. chrysogenum* genome, except that several putative *P. chrysogenum* pseudogenes in the locus appear to have been replaced with the *vrt* cluster. The *gsf* cluster consists of 13 putative genes (designated as *gsfA-K*, *gsfR1*, and *gsfR2*) and was found inserted between *orf4′* and *orf5′*, which are highly similar to Pc06 g01020 and Pc06 g01000 (92% and 94% identity, respectively). The *gsf* cluster replaces Pc06 g01010 in the *P. chrysogenum* genome (Figure 4B and Table 2). The genes immediately flanking the *gsf* cluster also remained syntenic with the corresponding locus in the *P. chrysogenum* genome. These observations of *vrt* and *gsf* clusters embedded within conserved syntenic regions led to speculation that *P. aethiopicum* may have acquired the two gene clusters via horizontal gene transfer (Walton, 2000). However, careful examinations of the Pc00c21 and Pc00c06 contigs revealed the presence of small conserved regions (some annotated as pseudogenes),

Table 2. Putative Genes Within and Flanking the *gsf* Cluster

Gene	Size (bp/aa)	BLASTP homolog	Identity/ Similarity (%)	Conserved Domain	E value
gsfA	5672/1790	*B. fuckeliana*, PKS14 *A. terreus*, ATEG_08451 (ACAS)	57/71 42/60	SAT-KS-MAT-PT-ACP	
gsfB	1442/419	*P. marneffei*, PMAA_079120 *G. fujikuroi*, Bik3 bikaverin *O*-methyltransferase[3]	41/61 29/45	pfam00891, *O*-methyltransferase COG2226, UbiE, Methylase involved in ubiquinone/menaquinone biosynthesis	7e-33 9e-07
gsfC	1191/396	*N. hematococca*, NECHADRAFT_81295 *A. flavus, omtB* aflatoxin *O*-methyltransferase[4]	32/51 24/44	pfam00891, *O*-methyltransferase	2e-20
gsfD	378/1301	*P. chrysogenum*, Pc12 g06140 *A. flavus, omtB* aflatoxin *O*-methyltransferase[4]	26/41 27/45	pfam00891, *O*-methyltransferase	1e-21
gsfE	1134/377	*A. nidulans*, AN9028.2	61/74	COG0451, WcaG, Nucleoside-diphosphate-sugar epimerases/ dehydratases	1e-09
gsfF	1603/462	*N. hematococca*, NECHADRAFT_3047	37/53	pfam00067, p450, Cytochrome P450	2e-37
gsfG	1033/299	*C. globosum*, CHGG_02201	24/37	cd00204, ANK, ankyrin repeats; ankyrin repeats mediate protein-protein interactions	7e-37
gsfH	889/237	*A. oryzae*, AO090001000095	81/89	cd01012, YcaC_related, YcaC related amidohydrolases	1e-31
gsfI	1976/533	*C. chiversii*, RadH flavin-dependent halogenase	61/75	pfam04820, tryptophan halogenase COG0644, FixC, dehydrogenases (flavoproteins)	3e-15 3e-17
gsfJ	2031/554	*A. nidulans*, AN8459.2	47/61	TIGR00711, efflux_EmrB, drug resistance transporter, EmrB/QacA subfamily	1e-24
gsfK	1028/251	*P. chrysogenum*, Pc12 g16460	40/59	PRK06953, short chain dehydrogenase	4e-24
gsfR1	2118/688	*A. nidulans*, AN8460.2	52/68	pfam04082, fungal specific transcription factor domain	2e-05
gsfR2	1248/415	*Sclerotinia sclerotiorum*, SS1G_05579	53/67	smart00066, GAL4-like Zn(II)2Cys6 binuclear cluster DNA-binding domain	8e-09
orf1′	1246/351	*P. chrysogenum*, Pc06 g01050	86/90	No conserved domain detected	
orf2′	1310/366	*P. chrysogenum*, Pc06 g01040	96/99	cd03445, Thioesterase II repeat2 cd03444, Thioesterase II repeat1	7e-27 2e-20
orf3′	765/211	*P. chrysogenum*, Pc06 g01030	80/86[a]	No conserved domain detected	
orf4′	2187/653	*P. chrysogenum*, Pc06 g01020	92/96	PRK08310, amidase	4e-30
orf5′	2352/783	*P. chrysogenum*, Pc06 g01000	94/96	pfam04082, fungal specific transcription factor domain	2e-16
orf6′	807/157	*P. chrysogenum*, Pc06 g00990	90/94	No conserved domain detected	
orf7′	1346/411	*P. chrysogenum*, Pc06 g00980	94/96	pfam07942, N2227-like protein	1e-85
orf8′	2268/702	*P. chrysogenum*, Pc06 g00970	98/98	COG0443, DnaK, Molecular chaperone	2e-17

Genus abbreviation: A., *Aspergillus*; B., *Botryiotinia*; C., *Chaetomium*; G., *Giberrella*; N.. *Nectria*; P., *Penicillium*.
[a] Based on Pc06 g01030 conceptual translation as predicted by FGENESH, different from the version in GenBank.

which appeared to be fragments of *vrt* and *gsf* gene clusters, in the corresponding loci in *P. chrysogenum* (Figure 4). This finding suggests that *P. chrysogenum* may have possessed the *vrt* and *gsf* gene clusters in the past but have lost them during evolution.

Both clusters have two transcription factors (*vrtR1* and *vrtR2*, and *gsfR1* and *gsfR2*) that contain Zn(II)2Cys6 DNA-binding domains, which are similar to pathway-specific regulators such as *aflR* and *ctnA* for aflatoxin and citrinin biosynthesis, respectively (Ehrlich et al., 1999; Shimizu et al., 2007). It is unclear whether both or only one of the transcription factors is involved in the regulation of the corresponding cluster.

The Putative Biosynthetic Pathways for the Biosynthesis of Viridicatumtoxin

Previous isotope incorporation study showed that the biosynthesis of the tetracyclic carboxamide core of **1** is significantly different from tetracyclines in bacteria (de Jesus et al., 1982), including (1) differences in the cyclization regioselectivity of the carbon backbone (Thomas, 2001), (2) the nonacetate origin of C3, and (3) the retention of the oxygen at C4a of **1** from [1-^{13}C^{18}O]-acetate. These differences exclude the participation of a fully aromatic tetracene intermediate, such as the pretetramid intermediate in oxytetracycline biosynthesis (Thomas and

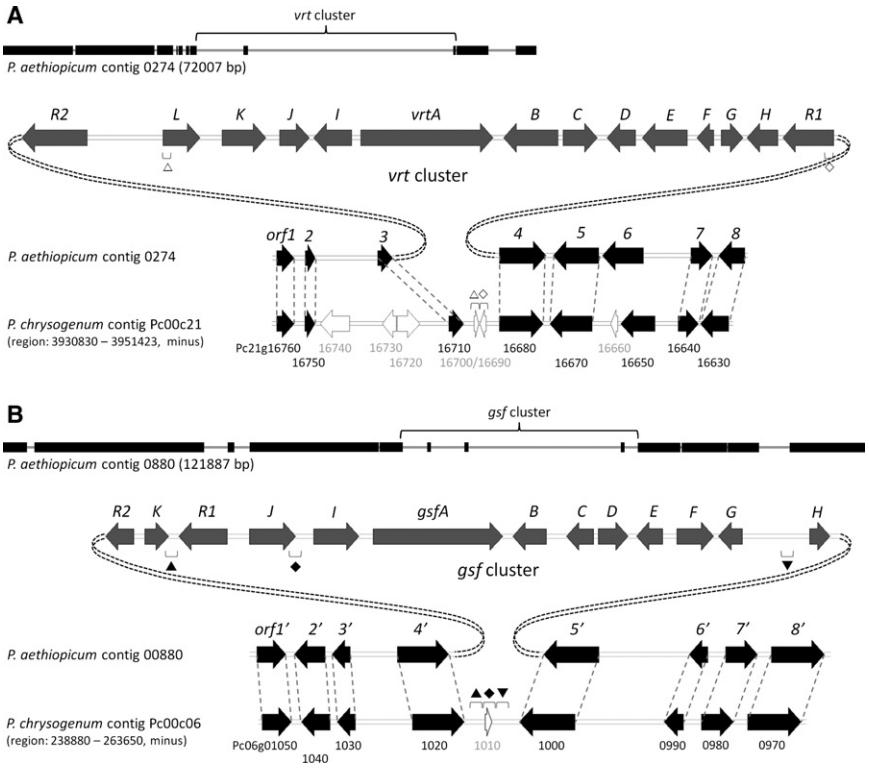

Figure 4. Putative *vrt* and *gsf* Clusters Embedded Within Conserved Syntenic Regions of *P. aethiopicum* Genome

(A) *vrt* cluster on contig 0274 and the corresponding locus on *P. chrysogenum* contig Pc00c21.

(B) *gsf* cluster on contig 0880 and the corresponding locus on *P. chrysogenum* contig Pc00c06. Blocks on the thin lines indicate conserved syntenic blocks on the contigs. The symbols (Δ ◇ ▲ ◆ ▼) indicate short conserved regions within the *vrt* and *gsf* clusters that are remained at the corresponding loci in *P. chrysogenum*. Block arrows: black, genes predicted not to be involved in the biosynthesis of **1** and **2;** white, putative pseudogenes.

Williams, 1983; Zhang et al., 2007). On the basis of the acetate labeling pattern and the new gene cluster data, a putative pathway for biosynthesis of **1** can be envisioned (Figure 5). The PT domain of a NRPKS has recently been shown to mediate aromatic polyketide cyclization (Crawford et al., 2009). Because the PT domain of VrtA shares high similarity to those from AptA and ACAS (61% and 50% identity), which were shown to produce polyketide products with C6-C11 first-ring cyclization regioselectivity, we reasoned that the cyclization of the polyketide backbone of **1** by VrtA may also proceed via a similar route. We hypothesized that VrtA may utilize a malonamoyl-CoA starter unit, which is generated by VrtB, followed by sequential condensation of eight malonyl-CoA units to form the polyketide backbone. The cyclizations of the BCD rings were assumed to follow the pattern observed in atrochrysone biosynthesis (Awakawa et al., 2009), in which the oxygen at C4a is retained from an acetate unit (Figure 5). Cyclization of the last ring (ring A) along with offloading of the intermediate **5** could be mediated by VrtG, which has protein sequence similarity to the recently discovered β-lactamase-type TE (AptB and ACTE, 60% and 49% protein identity) (Awakawa et al., 2009; Szewczyk et al., 2008).

The hypothesis of a malonamoyl-CoA starter unit produced by VrtB is supported by the high sequence similarity of VrtB to acetoacetyl-CoA synthetases (AACSs) (44% protein identity with the rat homolog, AACS_RAT), and the structural similarity of the AACS substrate, acetoacetate, to malonamate. AACS activates acetoacetate as an acyl-AMP intermediate followed by ligation to the free thiol of CoA to form acetoacetyl-CoA (Fukui et al., 1982). Similarly, the formation of malonamoyl-CoA from malonamate could be catalyzed by VrtB. Furthermore, *P. aethiopicum* has an additional copy of putative AACS gene (PaAACS1086) on contig1086, which is 96% identical to the only AACS homolog (Pc13 g10810) in *P. chrysogenum*, whereas VrtB shares only 50% protein identity with the putative PcAACS (Pc13 g10810). This implies that VrtB is most likely dedicated to the *vrt* pathway, whereas PaAACS1086 is involved in the primary metabolism.

VrtJ has a pyridoxal 5′-phosphate (PLP)–binding site and a conserved domain similar to those found in threonine aldolase (TA), aspartate aminotransferase and β-eliminating lyase (Table 1). The closest characterized homolog of VrtJ is Gly1 from *Candida albicans* (39% protein identity), which is a TA that catalyzes degradation of L-threonine to glycine and acetaldehyde (McNeil et al., 2000). The presence of an additional copy of TA-like gene (PaTA0310) in *P. aethiopicum*, which shares higher identity (92%) to the only homolog in *P. chrysogenum* (Pc12 g01020) than VrtJ (54%), again implies that PaTA0310 is most likely to be the primary TA involved in glycine metabolism. VrtJ is therefore likely to be dedicated to the *vrt* pathway and may be involved in the synthesis of the malonamate substrate for VrtB. A malonamoyl-CoA starter unit is also likely involved in oxytetracyline biosynthesis; however, the malonate-derived carboxamide of oxytetracyline is in contrast to the acetate-derived carboxamide of **1** (Thomas and Williams, 1983). One possibility could be a malonamoyl-CoA starter derived from asparagine, presumably synthesized by VrtJ and VrtB collaboratively (Figure 5). Such a pathway, however, does not match the previous acetate labeling study because incorporation of an asparagine-derived malonamoyl-CoA would result in the C3 of **1** being labeled by the C2 of [1,2-^{13}C]-acetate. This is because asparagine originates from oxaloacetate, and the formation of oxaloacetate from [1,2-$^{13}C_2$]-acetate proceeds via a symmetrical succinate intermediate in the tricarboxylic acid cycle (Ogasawara and Liu, 2009). Further gene targeting along with biochemical characterization of the four gene products, VrtA/B/G/J, are likely to shed light to the enzymatic reactions involved in the biosynthesis of the tetracyclic carboxamide core.

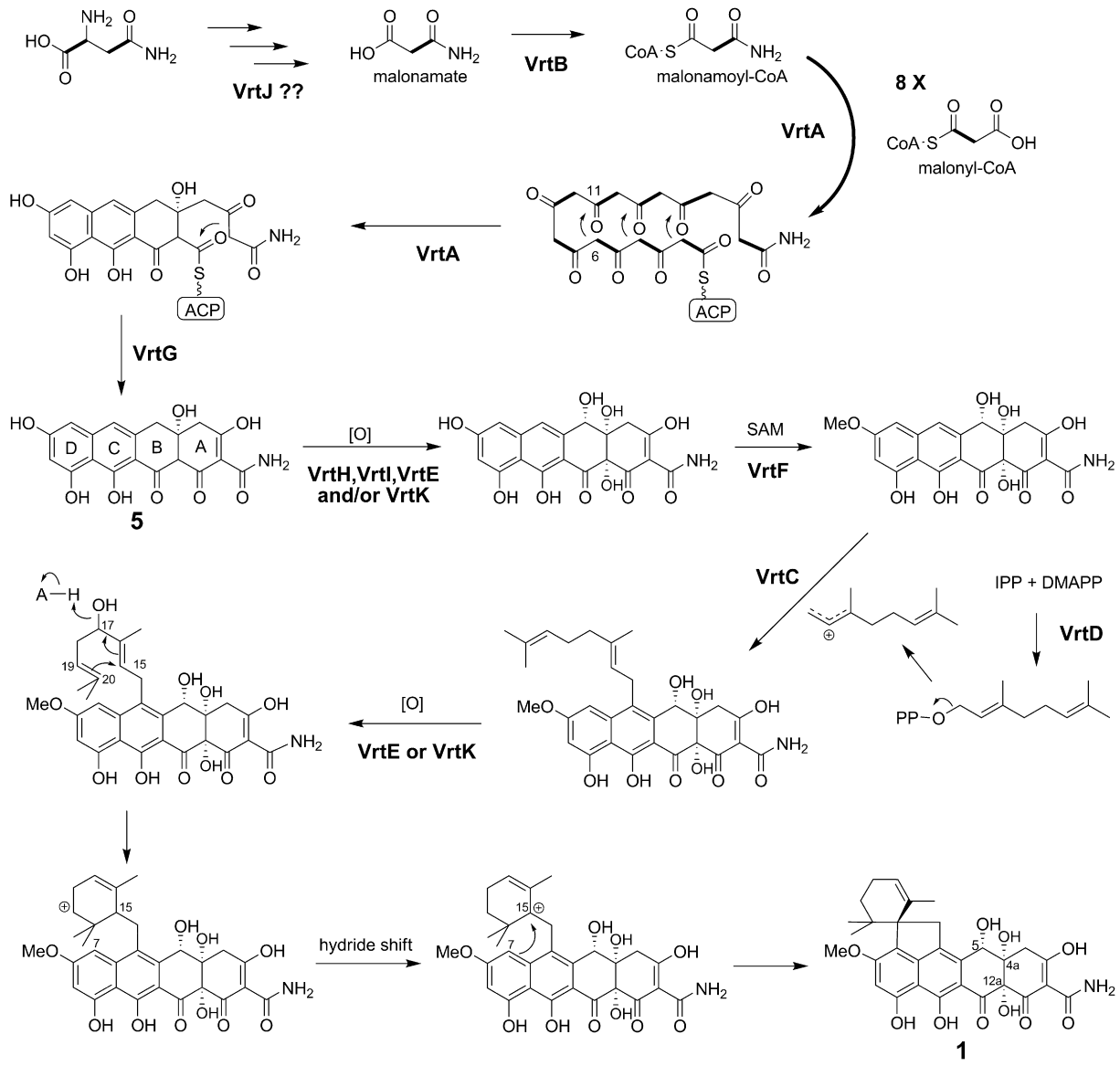

Figure 5. Proposed Pathway for the Biosynthesis of Viridicatumtoxin 1
DMAPP, dimethylallyl pyrophosphate; IPP, isopentenyl pyrophosphate.

The proposed post-PKS tailoring steps following the formation of intermediate **5** are two hydroxylations and an *O*-methylation (Figure 5). The hydroxylations at C5 and C12a are predicted to be catalyzed by one or two of the oxygenases (VrtH, VrtI, VrtE, and VrtK), whereas the methoxy group is likely to be formed by the *O*-methyltransferase (VrtF). The pathway that leads to formation of the spirobicyclic ring of **1** is proposed to involve at least three gene products in the cluster (Figure 5). VrtD, which is similar to *trans*-isoprenyl diphosphate synthases (Table 1), such as the *Neurospora crassa* farnesyl pyrophosphate synthase (Homann et al., 1996), is predicted to catalyze the formation of geranylpyrophosphate. On the basis of the shared homology of VrtC with aromatic prenyltransferases, such as *A. fumigatus* dimethylallyltryptophan synthase FgaPT2 (Metzger et al., 2009) (Table 1), the protein is predicted to catalyze the attachment of the geranyl moiety to the C ring of **1** to yield **6** (Figure 5). Most aromatic prenyltransferases identified in fungi transfer the prenyl group to a tryptophan or indole moiety (Heide, 2009). Intriguingly, VrtC is proposed to catalyze the transfer of a geranyl group to the aromatic C ring of the tetracyclic polyketide intermediate of **1**. Prenylation at the same C6 position is also observed in a similar fungal tetracyclic compound, hypomycetin, which has an acetyl group in place of the carboxamide in **1** (Breinholt et al., 1997). Thus, VrtC and the corresponding prenyltransferase in hypomycetin pathway can be considered as potential enzymes that can modify tetracycline compounds at C6.

We propose that the cyclization of the geranyl moiety of **6** can be initiated by a cytochrome P450 enzyme-catalyzed hydroxylation (VrtE or VrtK) at the allylic C17, which upon protonation of the hydroxyl can lead to a C17 carbocation (Figure 5). Attack

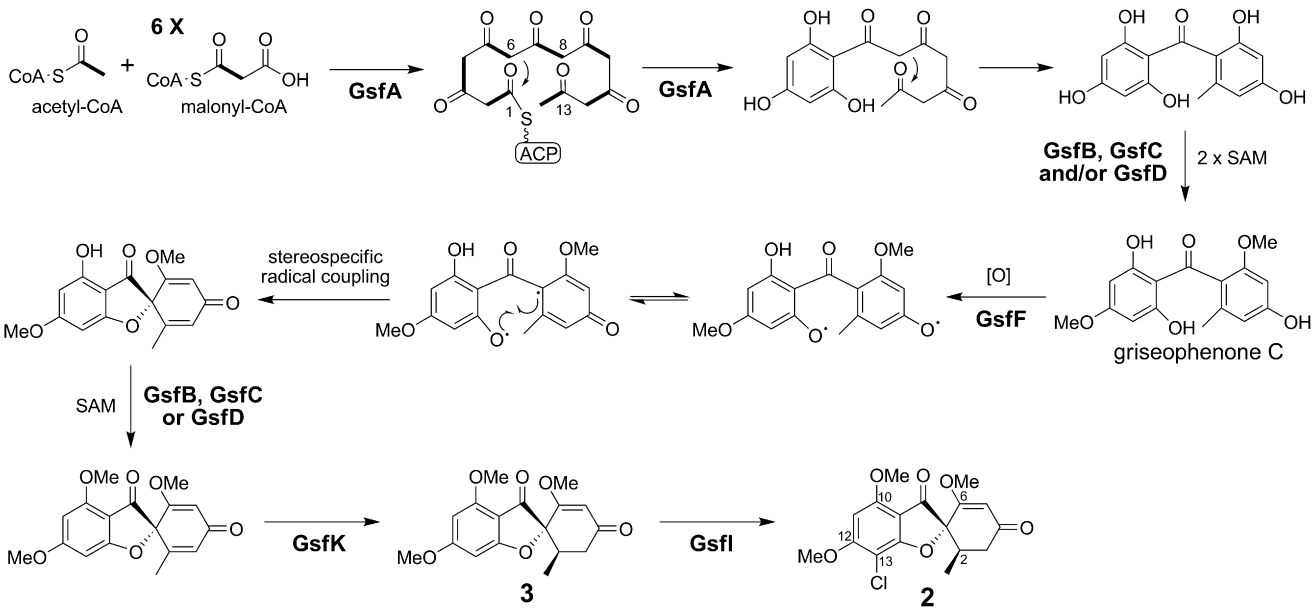

Figure 6. Proposed Biosynthesis of Griseofulvin 2
The function of the halogenase GsfI has been confirmed using knockout as shown in Figure 2.

of C20 on the bridging C15 forms the C15-C20 bond and transfers the positive charge to C19. A hydride shift from C15 to C19 is followed by C7 attack on C15 to form the spirobicyclic ring (Figure 5). The 1,3-hydride shift was previously proposed to rationalize the incorporation pattern of ^{2}H-labeled mevalonate (Horak et al., 1988). The cyclization of the geranyl side chain to the spirobicyclic ring in **1** is most likely enzyme mediated; however, no terpene cyclase gene is found in the vicinity of the *vrt* cluster. Thus, formation of the spirobicyclic ring in **1** could be mediated by the prenyltransferase (VrtC) as similarly proposed in paspaline biosynthesis (Saikia et al., 2006) or facilitated by the P450 enzyme.

The Putative Biosynthetic Pathway for the Biosynthesis of Griseofulvin

The biosynthesis of **2**, as implied by the previously established pathway (Harris et al., 1976), required at least seven biosynthetic enzymes (Figure 6 and Table 2). Formation of the heptaketide backbone by GsfA is initiated by priming with acetyl-CoA, followed by sequential condensations of six malonyl-CoA units (Simpson and Holker, 1977). Because neither a fused TE/CLC nor a stand-alone TE is present, we proposed that the C1-C6 Claisen cyclization of the polyketide backbone could be mediated by the PT domain of GsfA, whereas the C8-C13 aldol cyclization could occur spontaneously to afford the benzophenone intermediate of **2** (Figure 6). Alternatively, the PT domain may mediate the cyclization of both aromatic rings. Because PT domains of fungal PKSs are so far known to only catalyze aldol cyclizations (Crawford et al., 2009), the mechanism of folding and cyclization of the polyketide backbone by GsfA requires further investigation.

An isotope feeding experiment by Harris et al. (1976) established that two of the *O*-methylation steps at C6 and C12 hydroxyl groups occur immediately after the formation of the benzophenone intermediate to yield griseophenone C, whereas the methylation of the hydroxyl group at C10 occurs at a later stage (Figure 6). Three *O*-methyltransferases (GsfB/C/D) are encoded in the gene cluster and can therefore catalyze the required methylation steps.

An interesting feature in the biosynthesis of **2** is the formation of the heterocyclic ring by a stereospecific phenol oxidative coupling, which leads to the unique spiro structure of **2**. Geodin is another grisan compound similar to **2**, which also undergoes a similar stereospecific oxidative coupling. It has been established that the *A. terreus* dihydrogeodin oxidase (DHGO), which converts the benzophenone dihydrogeodin to (+)-geodin, is a multicopper blue protein similar to laccases (Fujii et al., 1987; Huang et al., 1995). The structural similarity of **2** to geodin suggests that a similar enzyme may be responsible for the oxidative coupling reaction, but no such enzyme is encoded in the *gsf* cluster. A P450 oxygenase (GsfF) was found in the *gsf* cluster, although no oxidation is required en route to **2**. We proposed that GsfF may catalyze the stereospecific oxidative coupling reaction of griseophenone C to form the grisan core (Figure 6). Oxidative coupling reactions catalyzed by cytochrome P450 enzymes are not unprecedented. A well-known example is OxyB involved in the phenol coupling reaction during the biosynthesis of vancomycin (Zerbe et al., 2004). GsfK, a putative NAD(P)-dependent oxidoreductase, is likely to catalyze the stereospecific reduction step at the C-ring resulting in the *R* conformation at the C2, forming the second chiral center in **2** and **3** (Figure 6).

GsfI is a halogenase that shares high similarity (60% identity) to the recently discovered flavin-dependent chlorinase (RadH) in the biosynthesis of radicicol (Wang et al., 2008). In the current study, **3** is a major product in the *P. aethiopicum* culture when grown on stationary YMEG liquid culture, albeit often produced at a slightly lower ratio to **2**. To confirm the function of GsfI, the

gene was disrupted in the same manner as the two PKSs. Two positive *gsf*I disruptants, Δ*gsfI*-IV5 and Δ*gsfI*-IV11, were found after screening approximately 100 glufosinate-resistant transformants. LC-MS analysis showed that disruption of *gsf*I completely abolished the production of **2**, whereas production of **3** remained (Figure 2). This finding confirmed the role of GsfI as a halogenase responsible for the regiospecific chlorination of **3** at the C13 position to form **2.** The result also suggests that chlorination does not affect the formation of the grisan ring and could therefore be one of the last steps in the **2** biosynthetic pathway in *P. aethiopicum* (Figure 6).

In conclusion, we have successfully associated two polyketide products to their corresponding gene clusters by bioinformatics and comparative analysis of the *P. aethiopicum* genome, and subsequently confirmed the functions of three of the biosynthetic genes by targeted gene replacement. As opposed to the previously reported low gene targeting efficiency in other *Penicillium* species (Casqueiro et al., 1999; Schumann and Hertweck, 2007), our results showed that gene targeting by double homologous recombination in *P. aethiopicum* is relatively feasible. The *P. aethiopicum* transformation system developed in this study will facilitate future mechanistic studies of the two pathways, as well as the numerous other PKSs found in the genome of this fungus.

SIGNIFICANCE

The present study unveiled the biosynthetic gene clusters of two interesting polyketide spiro compounds, 1 and 2; 1 is a rare example of fungal compound that is structurally similar to the tetracycline antibiotics from bacteria, whereas 2 is an important antifungal drug that has been in use for a long time for treating dermatophyte infections. Localization of the two gene clusters within conserved syntenic regions of the *P. aethiopicum* genome raises interesting questions regarding the evolution of clustering of secondary metabolite genes in fungi and may provide insights to the underlying genetic basis of *Penicillium* chemotaxanomy.

The *vrt* cluster is an interesting example of a biosynthetic pathway that encodes for a polyketide-isoprenoid hybrid compound in fungi. Understanding the exact mechanism by which the anhydrotetracycline-like core of 1 is formed by further targeted gene deletion and biochemical characterization of the gene products may provide new chemical insights. The unusual folding and cyclization of the isoprenoid moiety to form the spirobicylic ring also deserves further investigation. More importantly, unveiling the clustered genes for biosynthesis of 1 has opened up the possibilities to generate novel tetracycline analogs using combinatorial biosynthetic strategies by integrating bacterial and fungal genes that can act on the tetracycline scaffolds.

There has been a renewed interest in 2 owing to its newly discovered anticancer and antiviral properties. It is significant that this is the first report of the genetic basis of biosynthesis of 2. Further functional characterization of the gene cluster will advance our understanding of biosynthesis of 2 and could lead to isolation of intermediates that may have important implications in producing useful structural analogs either by enzymatic or chemical modifications.

EXPERIMENTAL PROCEDURES

Strains and Culture Conditions

P. aethiopicum, IBT 5753, was obtained from the IBT culture collection (Kgs. Lyngby, Denmark) and maintained on YMEG agar (4 g/l yeast extract, 10 g/l malt extract, and 16 g/l agar) or glucose minimal medium (GMM) (Cove, 1966) at 28°C.

454 Sequencing and Bioinformatic Analysis

The genomic DNA used for sequencing was prepared as described elsewhere (Gauch et al., 1998) from mycelium grown in stationary liquid culture. The shotgun sequencing was performed at the GenoSeq (UCLA Genotyping and Sequencing Core) with the GS FLX Titanium system (Roche).

The 454 sequencing reads were assembled into contigs with the GS De Novo Assembler software (Roche). The contigs were converted into BLAST database format for local BLAST search using stand-alone BLAST software (ver. 2.2.18) downloaded from the NCBI website. Gene predictions were performed using the FGENESH program (Softberry) and manually checked by comparing with homologous gene/proteins in the GenBank database. Functional domains in the translated protein sequences were predicted using Conserved Domain Search (NCBI) or InterproScan (EBI). Phylogenetic analysis was performed with MEGA4 software (Tamura et al., 2007).

Fungal Transformation and Gene Disruption in *P. aethiopicum*

Polyethylene glycol–mediated transformation of *P. aethiopicum* was done essentially as described previously for *A. nidulans* (Andrianopoulos and Hynes, 1988; Chooi et al., 2008), except that the protoplasts were prepared with 3 mg/mL lysing enzymes (Sigma-Aldrich) and 2 mg/mL Yatalase (Takara Bio). Construction of fusion PCR knockout cassettes containing the *bar* gene were performed as described elsewhere (Szewczyk et al., 2006), except that the homologous regions flanking the resistant marker were increased to 2 kb. Fusion PCR products were gel purified and sequenced before using for transformation. The *bar* gene with the *trp*C promoter was amplified from the plasmid pBARKS1 (Pall and Brunelli, 1993), which was obtained from the Fungal Genetics Stock Center (FGSC). RNA-silencing plasmids were constructed from pBARGPE1 (Pall and Brunelli, 1993) obtained from FGSC. Glufosinate used for the selection of *bar* transformants was prepared by extracting twice with equal volume of 1-butanol from commercial herbicide Finale (Bayer), which contains 11.33% (w/v) glufosinate-ammonium (Hays and Selker, 2000). The resulting aqueous phase was filter-sterilized and used directly at 40 μL/mL of GMM with 1.2 M sorbitol and 10 mM ammonium tartrate as the sole nitrogen source. Miniprep genomic DNA from *P. aethiopicum* transformants was used for PCR screening of gene deletants and was prepared as described elsewhere for *A. nidulans* (Chooi et al., 2008). Primers used for amplification of fusion PCR products and screening of transformants are listed in Table S2. Southern hybridizations were performed with DIG-High Prime DNA labeling and detection starter kit II (Roche Applied Science) following manufacturer's protocol.

Chemical Analysis and Compound Isolation

For small-scale analysis, the *P. aethiopicum* wild-type and transformants were grown in YMEG liquid medium (20 mL) for 7 days at 28°C without shaking. The cultures were extracted with equal volume of ethyl acetate and evaporated to dryness. The dried extracts were dissolved in methanol for LC-MS analysis. LC-MS was conducted with a Shimadzu 2010 EV Liquid Chromatography Mass Spectrometer by using both positive and negative electrospray ionization and a Phenomenex Luna 5 μL 2.0 × 100 mm C18 reverse-phase column. Samples were separated at a flow rate of 0.1 mL/min on a linear gradient of 5 to 95% solvent B in 30 min followed by isocratic 95% solvent B for another 15 min (solvent A: 0.1% (v/v) formic acid, solvent B: CH_3CN with 0.1% (v/v) formic acid). The identity of **1** and **2** were confirmed by comparing the UV spectra, retention time and *m/z* value to the authentic standards: **1** (a gift from Dr. Won-gon Kim, Korea Research Institute of Bioscience & Biotechnology) and **2** (Sigma-Aldrich).

Dechlorogriseofulvin was isolated using a solvent-solvent partitioning scheme as described elsewhere (Hutchison et al., 1973) followed by crystallization in MeOH. Briefly, the ethyl acetate extract from a two liters stationary liquid culture of a Δ*gsfI* mutant was evaporated to dryness and partition

between $CHCl_3/H_2O$. The $CHCl_3$ layer was further partitioned with hexane/MeOH (90%). The 90% MeOH layer was dried completely and redissolved in a small volume of MeOH (1 mL). Formation of white crystals, which was later confirmed to be **3**, was observed when the MeOH extract was left undisturbed at room temperature (further crystallized at 4°C). The crystals (28 mg) were collected by filtration, washed in cold methanol and dried. Purity of the compound was checked by LC-MS and the structure was confirmed by NMR with reference to published spectra (Table S3).

ACCESSION NUMBERS

The sequence of the *vrt* gene cluster (Table 1) was submitted to GenBank under the accession number GU574477. The sequence of the *gsf* gene cluster (Table 2) was submitted to GenBank under the accession number GU574478.

SUPPLEMENTAL INFORMATION

Supplemental Information includes three figures and three tables and can be found with this article online at doi:10.1016/j.chembiol.2010.03.015.

ACKNOWLEDGMENTS

We are grateful to W.G. Kim (Korea Research Institute of Bioscience & Biotechnology) for providing a standard of **1**. We thank W. Zhang for initial identification of **1** from *P. aethiopicum*; X. Xie and W. Xu for assistance with NMR of **3**; and John Vederas and Neil Garg for helpful discussions. We also want to acknowledge the suggestions provided by a reviewer on the biosynthetic pathway of **1.** This project was supported by a David and Lucile Packard Fellowship and NIH (1R01GM085128).

Received: January 22, 2010
Revised: March 26, 2010
Accepted: March 30, 2010
Published: May 27, 2010

REFERENCES

Andrianopoulos, A., and Hynes, M.J. (1988). Cloning and analysis of the positively acting regulatory gene *amdR* from *Aspergillus nidulans*. Mol. Cell. Biol. *8*, 3532–3541.

Ariza, M.R., Larsen, T.O., Duus, J.O., and Barrero, A.F. (2002). *Penicillium digitatum* metabolites on synthetic media and citrus fruits. J. Agric. Food Chem. *50*, 6361–6365.

Awakawa, T., Yokota, K., Funa, N., Doi, F., Mori, N., Watanabe, H., and Horinouchi, S. (2009). Physically discrete β-lactamase-type thioesterase catalyzes product release in atrochrysone synthesis by iterative type I polyketide synthase. Chem. Biol. *16*, 613–623.

Barton, D., and Cohen, T. (1957). Some biogenetic aspects of phenol oxidation. In Festschrift Prof. Dr. Arthur Stoll (Birkhäuser Verlag: Basel), p. 117.

Bergmann, S., Schumann, J., Scherlach, K., Lange, C., Brakhage, A.A., and Hertweck, C. (2007). Genomics-driven discovery of PKS-NRPS hybrid metabolites from *Aspergillus nidulans*. Nat. Chem. Biol. *3*, 213–217.

Bok, J.W., Hoffmeister, D., Maggio-Hall, L.A., Murillo, R., Glasner, J.D., and Keller, N.P. (2006). Genomic mining for *Aspergillus* natural products. Chem. Biol. *13*, 31–37.

Breinholt, J., Jensen, G.W., Kjaerr, A., Olsen, C.E., and Rosendahl, C.N. (1997). Hypomycetin—an antifungal, tetracyclic metabolite from *Hypomyces aurantius*: production, structure and biosynthesis. Acta Chem. Scand. *51*, 855–860.

Casqueiro, J., Gutierrez, S., Banuelos, O., Hijarrubia, M.J., and Martin, J.F. (1999). Gene targeting in *Penicillium chrysogenum*: disruption of the *lys2* gene leads to penicillin overproduction. J. Bacteriol. *181*, 1181–1188.

Chiang, Y.-M., Szewczyk, E., Nayak, T., Davidson, A.D., Sanchez, J.F., Lo, H.-C., Ho, W.-Y., Simityan, H., Kuo, E., Praseuth, A., et al. (2008). Molecular genetic mining of the *Aspergillus* secondary metabolome: discovery of the emericellamide biosynthetic pathway. Chem. Biol. *15*, 527–532.

Chooi, Y.-H., Stalker, D.M., Davis, M.A., Fujii, I., Elix, J.A., Louwhoff, S.H.J.J., and Lawrie, A.C. (2008). Cloning and sequence characterization of a non-reducing polyketide synthase gene from the lichen *Xanthoparmelia semiviridis*. Mycol. Res. *112*, 147–161.

Clardy, J., Springer, J.P., Buechi, G., Matsuo, K., and Wightman, R. (1975). Tryptoquivaline and tryptoquivalone, two tremorgenic metabolites of *Aspergillus clavatus*. J. Am. Chem. Soc. *97*, 663–665.

Cove, D.J. (1966). The induction and repression of nitrate reductase in the fungus *Aspergillus nidulans*. Biochim. Biophys. Acta *113*, 51–56.

Cox, R.J. (2007). Polyketides, proteins and genes in fungi: programmed nanomachines begin to reveal their secrets. Org. Biomol. Chem. *5*, 2010–2026.

Crawford, J.M., Dancy, B.C.R., Hill, E.A., Udwary, D.W., and Townsend, C.A. (2006). Identification of a starter unit acyl-carrier protein transacylase domain in an iterative type I polyketide synthase. Proc. Natl. Acad. Sci. USA *103*, 16728–16733.

Crawford, J.M., Korman, T.P., Labonte, J.W., Vagstad, A.L., Hill, E.A., Kamari-Bidkorpeh, O., Tsai, S.-C., and Townsend, C.A. (2009). Structural basis for biosynthetic programming of fungal aromatic polyketide cyclization. Nature *461*, 1139–1143.

de Jesus, A., Hull, W., Steyn, P., van Heerden, F., and Vleggaar, R. (1982). Biosynthesis of viridicatumtoxin, a mycotoxin from *Penicillium expansum*. J. Chem. Soc. Chem. Commun. 902–904.

Ehrlich, K.C., Montalbano, B.G., and Cary, J.W. (1999). Binding of the C6-zinc cluster protein, AFLR, to the promoters of aflatoxin pathway biosynthesis genes in *Aspergillus parasiticus*. Gene *230*, 249–257.

Finkelstein, E., Amichai, B., and Grunwald, M.H. (1996). Griseofulvin and its uses. Int. J. Antimicrob. Agents *6*, 189–194.

Frisvad, J.C., and Samson, R.A. (2004). Polyphasic taxonomy of *Penicillium* subgenus *Penicillium*. A guide to identification of food and air-borne terverticillate Penicillia and their mycotoxins. In Studies in Mycology 49: *Penicillium* subgenus *Penicillium*: new taxonomic schemes, mycotoxins and other extrolites, R.A. Samson and J.C. Frisvad, eds. (Utrecht, The Netherlands: Centraalbureau voor Schimmelcultures), pp. 1–174.

Fujii, I., Iijima, H., Tsukita, S., Ebizuka, Y., and Sankawa, U. (1987). Purification and properties of dihydrogeodin oxidase from *Aspergillus terreus*. J. Biochem. *101*, 11–18.

Fujii, I., Watanabe, A., Sankawa, U., and Ebizuka, Y. (2001). Identification of Claisen cyclase domain in fungal polyketide synthase WA, a naphthopyrone synthase of *Aspergillus nidulans*. Chem. Biol. *8*, 189–197.

Fukui, T., Ito, M., and Tomita, K. (1982). Purification and characterization of acetoacetyl-CoA synthetase from *Zoogloea ramigera* I-16-M. Eur. J. Biochem. *127*, 423–428.

Gauch, S., Hermann, R., Feuser, P., Oelmuller, U., and Bastian, H. (1998). Isolation of nucleic acids using anion-exchange chromatography: Qiagen-tip based methods. In Molecular Tools for Screening Biodiversity, A. Karp, D.S. Ingram, and P.G. Isaac, eds. (London: Chapman and Hall), pp. 54–59.

Halo, L.M., Heneghan, M.N., Yakasai, A.A., Song, Z., Williams, K., Bailey, A.M., Cox, R.J., Lazarus, C.M., and Simpson, T.J. (2008). Late stage oxidations during the biosynthesis of the 2-pyridone tenellin in the entomopathogenic fungus *Beauveria bassiana*. J. Am. Chem. Soc. *130*, 17988–17996.

Harris, C., Roberson, J., and Harris, T. (1976). Biosynthesis of griseofulvin. J. Am. Chem. Soc. *98*, 5380–5386.

Hays, S., and Selker, E. (2000). Making the selectable marker *bar* tighter and more economical. Fungal Genet. Newsl. *47*, 107.

Heide, L. (2009). Prenyl transfer to aromatic substrates: genetics and enzymology. Curr. Opin. Chem. Biol. *13*, 171–179.

Hoffmeister, D., and Keller, N. (2007). Natural products of filamentous fungi: enzymes, genes, and their regulation. Nat. Prod. Rep. *24*, 393–416.

Homann, V., Mende, K., Arntz, C., Ilardi, V., Macino, G., Morelli, G., Böse, G., and Tudzynski, B. (1996). The isoprenoid pathway: cloning and characterization of fungal FPPS genes. Curr. Genet. *30*, 232–239.

Horak, R., Maharaj, V., Marais, S., Heerden, F., and Vleggaar, R. (1988). Stereochemical studies on the biosynthesis of viridicatumtoxin: evidence for

a 1,3-hydride shift in the formation of the spirobicyclic ring system. J. Chem. Soc. Chem. Commun. *1988*, 1562–1564.

Huang, K.X., Fujii, I., Ebizuka, Y., Gomi, K., and Sankawa, U. (1995). Molecular cloning and heterologous expression of the gene encoding dihydrogeodin oxidase, a multicopper blue enzyme from *Aspergillus terreus*. J. Biol. Chem. *270*, 21495–21502.

Hutchison, R.D., Steyn, P.S., and van Rensburg, S.J. (1973). Viridicatumtoxin, a new mycotoxin from *Penicillium viridicatum* Westling. Toxicol. Appl. Pharmacol. *24*, 507–509.

Ishimaru, T., Tsuboya, S., and Saijo, T. (1993). Tetracyclic compounds, its production and use thereof. Japanese Patent 06-040995.

Jarvis, B., Zhou, Y., Jiang, J., Wang, S., Sorenson, W., Hintikka, E., Nikulin, M., Parikka, P., Etzel, R., and Dearborn, D. (1996). Toxigenic molds in water-damaged buildings: dechlorogriseofulvins from *Memnoniella echinata*. J. Nat. Prod. *59*, 553–554.

Jin, H., Yamashita, A., Maekawa, S., Yang, P., He, L., Takayanagi, S., Wakita, T., Sakamoto, N., Enomoto, N., and Ito, M. (2008). Griseofulvin, an oral antifungal agent, suppresses hepatitis C virus replication in vitro. Hepatol. Res. *38*, 909–918.

Lane, M., Nakashima, T., and Vederas, J. (1982). Biosynthetic source of oxygens in griseofulvin. Spin-echo resolution of oxygen-18 isotope shifts in carbon-13 NMR spectroscopy. J. Am. Chem. Soc. *104*, 913–915.

McNeil, J., Flynn, J., Tsao, N., Monschau, N., Stahmann, K., Haynes, R., McIntosh, E., and Pearlman, R. (2000). Glycine metabolism in *Candida albicans*: characterization of the serine hydroxymethyltransferase (SHM1, SHM2) and threonine aldolase (GLY1) genes. Yeast *16*, 167–175.

Metzger, U., Schall, C., Zocher, G., Unsöld, I., Stec, E., Li, S., Heide, L., and Stehle, T. (2009). The structure of dimethylallyl tryptophan synthase reveals a common architecture of aromatic prenyltransferases in fungi and bacteria. Proc. Natl. Acad. Sci. USA *106*, 14309–14314.

Nayak, T., Szewczyk, E., Oakley, C.E., Osmani, A., Ukil, L., Murray, S.L., Hynes, M.J., Osmani, S.A., and Oakley, B.R. (2006). A versatile and efficient gene targeting system for *Aspergillus nidulans*. Genetics *172*, 1557–1566.

Ogasawara, Y., and Liu, H.W. (2009). Biosynthetic studies of aziridine formation in azicemicins. J. Am. Chem. Soc. *131*, 18066–18068.

Pall, M., and Brunelli, J. (1993). A series of six compact fungal transformation vectors containing polylinkers with multiple unique restriction sites. Fungal Genet. Newsl. *40*, 59.

Panda, D., Rathinasamy, K., Santra, M., and Wilson, L. (2005). Kinetic suppression of microtubule dynamic instability by griseofulvin: implications for its possible use in the treatment of cancer. Proc. Natl. Acad. Sci. USA *102*, 9878–9883.

Raju, M.S., Wu, G.S., Gard, A., and Rosazza, J.P. (2004). Microbial transformations of natural antitumor agents. 20. Glucosylation of viridicatumtoxin. J. Nat. Prod. *45*, 321–327.

Rebacz, B., Larsen, T., Clausen, M., Ronnest, M., Loffler, H., Ho, A., and Kramer, A. (2007). Identification of griseofulvin as an inhibitor of centrosomal clustering in a phenotype-based screen. Cancer Res. *67*, 6342–6350.

Rhodes, A., Somerfield, G.A., and Mcgonagle, M.P. (1963). Biosynthesis of griseofulvin: observations on the incorporation of (^{14}C)griseophenone C and (^{36}C)griseophenones B and A. Biochem. J. *88*, 349–357.

Rønnest, M., Rebacz, B., Markworth, L., Terp, A., Larsen, T., Krämer, A., and Clausen, M. (2009). Synthesis and structure-activity relationship of griseofulvin analogues as inhibitors of centrosomal clustering in cancer cells. J. Med. Chem. *52*, 3342–3347.

Saikia, S., Parker, E., Koulman, A., and Scott, B. (2006). Four gene products are required for the fungal synthesis of the indole-diterpene, paspaline. FEBS Lett. *580*, 1625–1630.

Samson, R.A., Seifert, K.A., and Frisvad, J.C. (2004). Phylogenetic analysis of *Penicillium* subgenus *Penicillium* using partial tubulin sequences. In Studies in Mycolgy 49: *Penicillium* subgenus *Penicillium*: new taxonomic schemes, mycotoxins and other extrolites, R.A. Samson and J.C. Frisvad, eds. (Utrecht, The Netherlands: Centraalbureau voor Schimmelcultures), pp. 175–200.

Schumann, J., and Hertweck, C. (2007). Molecular basis of cytochalasan biosynthesis in fungi: gene cluster analysis and evidence for the involvement of a PKS-NRPS hybrid synthase by RNA silencing. J. Am. Chem. Soc. *129*, 9564–9565.

Schümann, J., and Hertweck, C. (2006). Advances in cloning, functional analysis and heterologous expression of fungal polyketide synthase genes. J. Biotechnol. *124*, 690–703.

Shimizu, T., Kinoshita, H., and Nihira, T. (2007). Identification and *in vivo* functional analysis by gene disruption of *ctnA*, an activator gene involved in citrinin biosynthesis in *Monascus purpureus*. Appl. Environ. Microbiol. *73*, 5097–5103.

Simpson, T.J., and Holker, J.S.E. (1977). 13C-NMR studies on griseofulvin biosynthesis and acetate metabolism in *Penicillium patulum*. Phytochemistry *16*, 229–233.

Szewczyk, E., Nayak, T., Oakley, C.E., Edgerton, H., Xiong, Y., Taheri-Talesh, N., Osmani, S.A., and Oakley, B.R. (2006). Fusion PCR and gene targeting in *Aspergillus nidulans*. Nat. Protoc. *1*, 3111–3120.

Szewczyk, E., Chiang, Y., Oakley, C., Davidson, A., Wang, C., and Oakley, B. (2008). Identification and characterization of the asperthecin gene cluster of *Aspergillus nidulans*. Appl. Environ. Microbiol. *74*, 7607.

Tamura, K., Dudley, J., Nei, M., and Kumar, S. (2007). MEGA4: Molecular Evolutionary Genetics Analysis (MEGA) software version 4.0. Mol. Biol. Evol. *24*, 1596–1599.

Thomas, R. (2001). A biosynthetic classification of fungal and streptomycete fused-ring aromatic polyketides. ChemBioChem *2*, 612–627.

Thomas, R., and Williams, D. (1983). Oxytetracycline biosynthesis: mode of incorporation of [1-^{13}C]-and [1, 2-$^{13}C_2$]-acetate. J. Chem. Soc. Chem. Commun. *1983*, 128–130.

Walton, J.D. (2000). Horizontal gene transfer and the evolution of secondary metabolite gene clusters in fungi: an hypothesis. Fungal Genet. Biol. *30*, 167–171.

Wang, S., Xu, Y., Maine, E., Wijeratne, E., Espinosa-Artiles, P., Gunatilaka, A., and Molnár, I. (2008). Functional characterization of the biosynthesis of radicicol, an Hsp90 inhibitor resorcylic acid lactone from *Chaetomium chiversii*. Chem. Biol. *15*, 1328–1338.

Wong, S., Kullnig, R., Dedinas, J., Appell, K., Kydd, G., Gillum, A., Cooper, R., and Moore, R. (1993). Anthrotainin, an inhibitor of substance P binding produced by *Gliocladium catenulatum*. J. Antibiot. (Tokyo) *46*, 214–221.

Yamazaki, M., Fujimoto, H., and Okuyama, E. (1976). Structure determination of six tryptoquivaline-related metabolites from *Aspergillus fumigatus*. Tetrahedron Lett. *17*, 2861–2864.

Zerbe, K., Woithe, K., Li, D.B., Vitali, F., Bigler, L., and Robinson, J.A. (2004). An oxidative phenol coupling reaction catalyzed by OxyB, a cytochrome P450 from the vancomycin-producing microorganism. Angew. Chem. Int. Ed. Engl. *43*, 6709–6713.

Zhang, W., Watanabe, K., Wang, C.C.C., and Tang, Y. (2007). Investigation of early tailoring reactions in the oxytetracycline biosynthetic pathway. J. Biol. Chem. *282*, 25717–25725.

Zheng, C.-J., Yu, H.-E., Kim, E.-H., and Kim, W.-G. (2008). Viridicatumtoxin B, a new anti-MRSA agent from *Penicillium* sp. FR11. J Antibiot. (Tokyo) *61*, 633–637.